

Effect of $\text{Al}_2\text{O}_{3\text{sf}}$ addition on the friction and wear properties of $(\text{SiC}_p + \text{Al}_2\text{O}_{3\text{sf}})/\text{Al2024}$ composites fabricated by pressure infiltration

Hui Xu¹⁾, Gong-zhen Zhang¹⁾, Wei Cui¹⁾, Shu-bin Ren¹⁾, Qian-jin Wang²⁾, and Xuan-hui Qu¹⁾

1) Institute for Advanced Materials and Technology, University of Science and Technology Beijing, Beijing 100083, China

2) Shandong Yinguang Yuyuan Light Metal Precise Forming Co. Ltd., Linyi 273400, China

(Received: 14 September 2017; revised: 1 December 2017; accepted: 8 December 2017)

Abstract: Aluminum (Al) 2024 matrix composites reinforced with alumina short fibers ($\text{Al}_2\text{O}_{3\text{sf}}$) and silicon carbide particles (SiC_p) as wear-resistant materials were prepared by pressure infiltration in this study. Further, the effect of $\text{Al}_2\text{O}_{3\text{sf}}$ on the friction and wear properties of the as-synthesized composites was systematically investigated, and the relationship between volume fraction and wear mechanism was discussed. The results showed that the addition of $\text{Al}_2\text{O}_{3\text{sf}}$, characterized by the ratio of $\text{Al}_2\text{O}_{3\text{sf}}$ to SiC_p , significantly affected the properties of the composites and resulted in changes in wear mechanisms. When the volume ratio of $\text{Al}_2\text{O}_{3\text{sf}}$ to SiC_p was increased from 0 to 1, the rate of wear mass loss (K_m) and coefficients of friction (COFs) of the composites decreased, and the wear mechanisms were abrasive wear and furrow wear. When the volume ratio was increased from 1 to 3, the COF decreased continuously; however, the K_m increased rapidly and the wear mechanism became adhesive wear.

Keywords: aluminum matrix composites; silicon carbide particles; alumina short fibers; friction properties; wear properties; infiltration

1. Introduction

Lightweighting is an important method for improving the mobility and increasing the payload and stability of heavy vehicles. Based on this, lightweighting a brake drum, a significant part of the wheel end assembly and as unsprung weight unit, is considerably important for creating light weight, strong, stiff, wear-resistant, and vibration-dampened components and results in a decrease in the weight of heavy vehicles. A traditional brake drum is made of cast iron (Fe), steel, or a combination of both. These materials have relatively large specific gravities and low cooling abilities, which leads to a dramatic increase of the brake drum temperature resulting in failure during continuous braking. In contrast, aluminum (Al) matrix composites with an added reinforced phase have the advantages of small specific gravity, rapid heat conduction, and good wear resistance [1]. Therefore, high quality brake drums can be produced by replacing cast Fe with Al matrix composites.

The shape of the reinforcement phases in Al matrix

composites can be particles, whiskers, and long or short fibers [2–4]. Frequently-used reinforcing materials are silicon carbide (SiC), alumina (Al_2O_3), aluminum nitride (AlN), graphite, and diamond. Among the metal matrix composites (MMCs), SiC particulate-reinforced Al matrix composites are widely used as wear-resistant materials in modern industries [5]. Abhik *et al.* [6] evaluated the mechanical and wear properties of an Al2014–SiC-reinforced MMC used for brake pads and manufactured by powder metallurgy. They found that a 20wt% SiC particle (SiC_p)-reinforced Al matrix composite exhibited a higher wear rate than the one reinforced with 10wt% SiC_p because of its lower density. Wang and Song [7] fabricated Al_2O_3 fiber ($\text{Al}_2\text{O}_{3\text{f}}$) and SiC_p hybrid MMCs by the squeeze casting method. They found that wear resistance increased with an increase in Al_2O_3 fiber content at room temperature. However, the hybrid reinforced composites were anisotropic because the Al_2O_3 consisted of long fibers in an ordered arrangement. When the temperature increased, SiC_p did not enhance the wear resistance and a larger mass loss occurred in planar random-orientated MMCs

Corresponding author: Shu-bin Ren E-mail: sbren@ustb.edu.cn

© University of Science and Technology Beijing and Springer-Verlag GmbH Germany, part of Springer Nature 2018

compared to normally orientated ones. In this research, Al matrix composites with $\text{SiC}_p + \text{Al}_2\text{O}_{3\text{sf}}$ (Al_2O_3 short fiber) were prepared to replace traditional cast Fe in automotive brakes. Short-fiber Al_2O_3 was selected to increase abrasive resistance and avoid anisotropy.

Currently, there are several methods for the manufacture of composites, including powder metallurgy [8], stir casting [9], and infiltration [10]. Comparison of these methods indicates that the infiltration process can realize the near net-shaped formation of high volume fraction particle-reinforced MMCs [11–13]. In this study, $\text{Al}_2\text{O}_{3\text{sf}}$ was added to SiC particles as part of the reinforcement phase, and $(\text{SiC}_p + \text{Al}_2\text{O}_{3\text{sf}})/\text{Al2024}$ composites (PFMMCs) were fabricated using the infiltration process. In addition, the influence of $\text{Al}_2\text{O}_{3\text{sf}}$ addition on the friction wear properties of the composites was systematically investigated.

2. Experimental

2.1. Preparation of materials

In this study, abrasive-grade green α -SiC particles of approximately 14 μm in diameter were used, as shown in Fig. 1(a). The diameter of the Al_2O_3 fibers was about 10 μm and the ratio of length to diameter was 5–10, as shown in Fig. 1(b). All the ceramic powders were subjected to etch washing and alkaline cleaning prior to use. The specific changes in the volume fractions of the reinforcement phases are listed in Table 1.

Al2024 alloys were used as the matrix material. Resol phenolic resin was used as the forming binder for the reinforcement particles. To avoid cracking of the green body during debinding, graphite particles (5–30 μm), as an auxiliary

forming additive, were added to replace a part of the forming binder during mixing of the reinforcement phase, which consisted of SiC_p and $\text{Al}_2\text{O}_{3\text{sf}}$ with the forming binder alnovol. In addition, aluminum dihydrogen phosphate ($\text{Al}(\text{H}_2\text{PO}_4)_3$), at 3vol% of the mixture, was added as a sintering aid into the mixture of SiC_p and $\text{Al}_2\text{O}_{3\text{sf}}$ to reduce the calcination temperature of the preform from 1800 to 1050°C. The pressure infiltration process was adopted for the preparation of PFMMCs.

The detailed process procedures are as follows. First, the mixtures consisting of SiC_p , $\text{Al}_2\text{O}_{3\text{sf}}$, 3vol% $\text{Al}(\text{H}_2\text{PO}_4)_3$, 19vol% graphite of three sizes, and 38vol% resol were thoroughly mixed for 1 h, and then put into a mold (its diameter $d = 60$ mm) and pressed for 0.5 h under a pressure of 20 MPa and a temperature of 200°C. The total volume fraction of SiC_p and $\text{Al}_2\text{O}_{3\text{sf}}$ was 40% and their specific ratios are listed in Table 1. A green body (60 mm in diameter \times 10 mm in thickness) was obtained and transferred to a furnace for debinding and calcination, during which the resol and graphite particles were removed. The calcination temperature was 1050°C. Thus, a porous preform was obtained. Subsequently, both the preform and the moderate Al alloys were placed into the infiltration equipment and heated to 750°C. The melted Al alloys infiltrated into the pores of the preform under a pressure of 10–15 MPa. This resulted in well-prepared Al composites with $\text{SiC}_p + \text{Al}_2\text{O}_{3\text{sf}}$. All the samples were subjected to solution treatment at 495°C for 90 min followed by water quenching. Then, aging was performed at 190°C for 12 h. A schematic illustration of the pressure infiltration process is shown in Fig. 2(a). A typical microstructure of the PFMMCs is shown in Fig. 2(b). Clearly, the $\text{Al}_2\text{O}_{3\text{sf}}$ - and SiC-reinforced phases are distributed randomly and uniformly in the matrix.

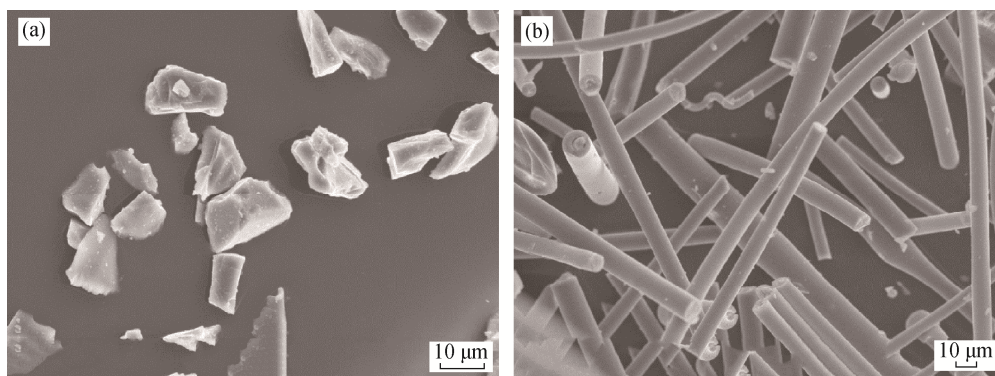


Fig. 1. SEM micrographs of (a) SiC_p and (b) $\text{Al}_2\text{O}_{3\text{sf}}$.

Table 1. Composition of PFMMCs vol%

No.	$\text{Al}_2\text{O}_{3\text{sf}}$	SiC_p	Al2024
1	0	40	60
2	10	30	60
3	20	20	60
4	30	10	60

2.2. Experimental conditions

Schematic view of the wear test is shown in Fig. 3(a) and the wear track on the worn disk surface is shown in Fig. 3(b). A sliding wear test was conducted using a 10 mm diameter pin against the PFMMCs discs, under dry

conditions. The pin was made of HT400 material, which is currently used for brake discs. The normal pressure and linear sliding velocities were 0.7 MPa and 0.5 m·s⁻¹, respectively. The experimental parameters were based on the requirements of actual situations in brake systems. The friction and wear tests were performed on a UMT-3

controlled environment friction wear test machine. The surface profile of the composites and the friction couplings were observed using a LEO-1450 scanning electron microscope, and the surface micro-topography was measured using a profile meter. All data represent the average of three tests.

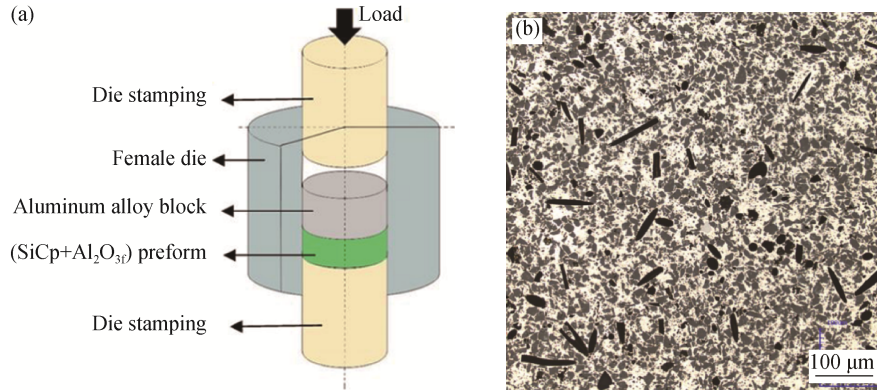


Fig. 2. Schematic illustration of the pressure infiltration process (a) and the typical microstructure of PFMMCs (b).

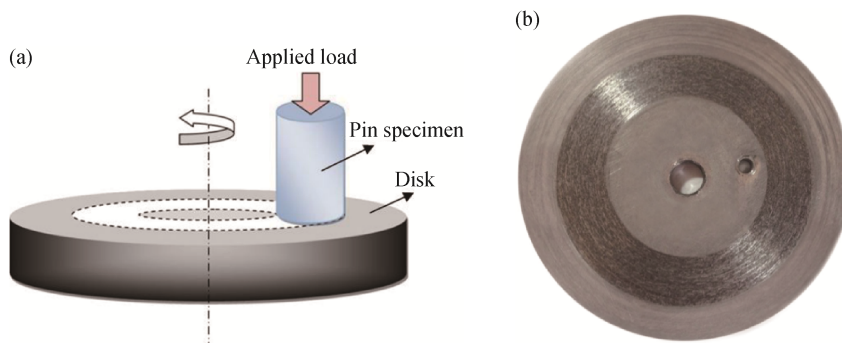


Fig. 3. Schematic view of the pin specimen and disk (a) and wear track on the worn disk surface (b).

3. Results and discussion

3.1. The rate of wear loss in composites fabricated from four volume fraction ratios of Al₂O_{3sf} to SiC_p

The rate of wear mass loss (K_m) is an important indicator for evaluating the wear-resistant properties of materials. For the composites fabricated in this study, K_m was calculated by

$$K_m = \frac{\Delta m}{L \cdot A_n} \tag{1}$$

where Δm is the wear loss value in mass, L is the relative sliding distance, and A_n is the contact area. The contact area A_n is $7.9 \times 10^{-5} \text{ m}^2$. All data represent the average of three tests.

Fig. 4 shows the variation in K_m for different materials. Clearly, when the volume ratio of Al₂O_{3sf} to SiC_p is 1:1, the K_m of PFMMCs is reduced, while that of HT400 increases. Without the support of Al₂O_{3sf}, SiC_p in 40vol%SiC/Al2024

easily dropped off during the process of friction and wear, thus this sample, No. 1, exhibits a greater loss in mass. With an increase of Al₂O_{3sf} from 0vol% to 20vol%, the wear mass loss of the composites obviously drops and the wear resistance significantly improves. The wear loss values of the

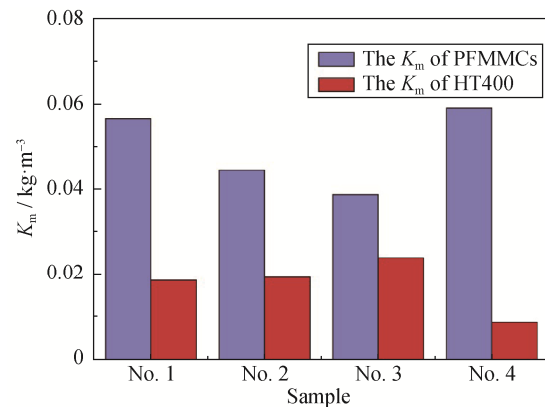


Fig. 4. K_m of the composites fabricated from four volume fraction ratios of Al₂O_{3sf} to SiC_p.

opposite friction elements (HT400) increase with improvements in the wear resistance of the composites. The K_m of PFMMCs increases suddenly from 39.01 to 59.34 when the ratio of $\text{Al}_2\text{O}_{3\text{sf}}$ to SiC_p is 3:1. Thus, the addition of an excessive amount of $\text{Al}_2\text{O}_{3\text{sf}}$ results in an increase in the rate of wear loss and worsens the abrasion characteristics.

3.2. Friction coefficient

Fig. 5 shows the variation in the coefficient of friction (COF) of the four samples. An initial running-in stage appears at the beginning of the examination and the COF increases to a maximum. The COF is seen to decrease with an increase in the volume fraction of $\text{Al}_2\text{O}_{3\text{sf}}$. The average COF of sample No. 4 is 0.37 and those of samples No. 1, 2, and 3 are 0.55, 0.50, and 0.48, respectively. As indicated by the arrows, a sudden drop appears in the COF curves of 40vol% $\text{SiC}_p/\text{Al2024}$, (10vol% $\text{Al}_2\text{O}_{3\text{sf}}$ + 30vol% SiC_p)/ Al2024 , and (20vol% $\text{Al}_2\text{O}_{3\text{sf}}$ + 20vol% SiC_p)/ Al2024 . However, in contrast, the curve of sample No. 4 shows a sudden increase. The heat conduction performance of $\text{Al}_2\text{O}_{3\text{sf}}$ is poorer than that of the SiC_p -reinforced Al matrix composite and the heat dissipation of the composites worsens with an increase in the volume fraction of $\text{Al}_2\text{O}_{3\text{sf}}$. Therefore, the local temperature increases rapidly due to the poor heat dissipation of the composite. Severe plastic deformation of the discs occurs easily in this high-temperature environment and the sudden increase in COF is attributed to plastic deformation between the surface of the pin and the disc. Here we speculate that the wear mechanism has changed.

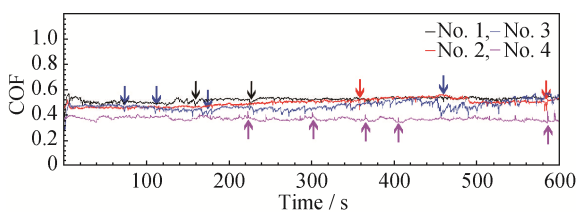


Fig. 5. Coefficients of friction of the composites fabricated from four volume fraction ratios of $\text{Al}_2\text{O}_{3\text{sf}}$ to SiC_p .

3.3. Worn surfaces of composites made from four volume fraction ratios of $\text{Al}_2\text{O}_{3\text{sf}}$ to SiC_p

Fig. 6 shows the microstructures of the composite surfaces after the pin-on-disc wear tests and the surface profiles of the samples are presented in Fig. 7. Abrasive wear and furrow wear are obvious in Figs. 6(a), 6(b), and 6(c). Clearly, the furrows become shallower with an increase in the volume fraction of $\text{Al}_2\text{O}_{3\text{sf}}$ in the porous preform. The reinforcement phases of PFMMCs, shown in Fig. 6(a), are all

granular, and in this case, the particles or Al alloy are easily desquamated from the PFMMCs. Thus, the reason for the sudden COF drop shown in Fig. 5 is a reduction in friction due to SiC_p as it easily flakes off from the matrix and causes sliding on the surface of composites. SiC_p broken off from the matrix becomes a hard abrasive and scored deep trenches into the surface of the PFMMCs, resulting in more and more alloy being worn away. The addition of $\text{Al}_2\text{O}_{3\text{sf}}$ with crossing structure and supportive characteristics made it more difficult for SiC_p to strip away from the matrix. Thus, the addition of $\text{Al}_2\text{O}_{3\text{sf}}$ can improve wear-resistant properties. As a result, the K_m of the composite 40vol% $\text{SiC}_p/\text{Al2024}$ was greater than that of (10vol% $\text{Al}_2\text{O}_{3\text{sf}}$ + 30vol% SiC_p)/ Al2024 and (20vol% $\text{Al}_2\text{O}_{3\text{sf}}$ + 20vol% SiC_p)/ Al2024 .

When $\text{Al}_2\text{O}_{3\text{sf}}$ and SiC_p were used in the volume ratio of 3:1, the wear mechanism exhibited a transition from abrasive to adhesive wear, as shown in Fig. 6(d). Fig. 7(d) shows that the breadth and depth of the furrows are larger than those in the other samples, and Fig. 4 shows that the K_m of (30vol% $\text{Al}_2\text{O}_{3\text{sf}}$ + 10vol% SiC_p)/ Al2024 is the greatest of all.

Adhesive wear easily occurs because of the inter-solubility between Al and Fe. However, SiC_p could increase the rheological strength of metals [14] and slow down the formation and/or propagation of cracks. Moreover, the flaking off of SiC_p from the matrix reduces the possibility of adhesive wear. Therefore, it is reasonable that plowing and abrasive wear were dominant when the volume ratios of $\text{Al}_2\text{O}_{3\text{sf}}$ to SiC_p of 0, 1:3, and 1:1 were used. When the volume ratio of $\text{Al}_2\text{O}_{3\text{sf}}$ to SiC_p was 3:1, the thermal conductivity was the lowest. As a result, the composites were welded by friction coupling because of the elevated temperature. The just-formed joint points were clipped in the subsequent sliding process, forming obvious corrugations and plastic tearing features. When adhesion occurred, the COF increased suddenly, as indicated by the arrows in the curve of sample No. 4, shown in Fig. 4.

Figs. 8 and 9 show elemental iron on the surface of the composites and elemental aluminum and silicon on the surface of the friction-coupled HT400. The composite layer, characterized by rich Fe, was formed by wear debris ground from HT400. These Fe filings stick to the contacting surfaces of friction pairs and form a dense alloy layer, containing SiC and Al_2O_3 , by mechanical alloying [15–16]. At the same time, an alloy layer was detected on the surface of HT400. The worn surfaces of PFMMCs are mainly composed of Al, SiC, Al_2O_3 , and Fe, as indicated by the XRD spectrum shown in Fig. 10.

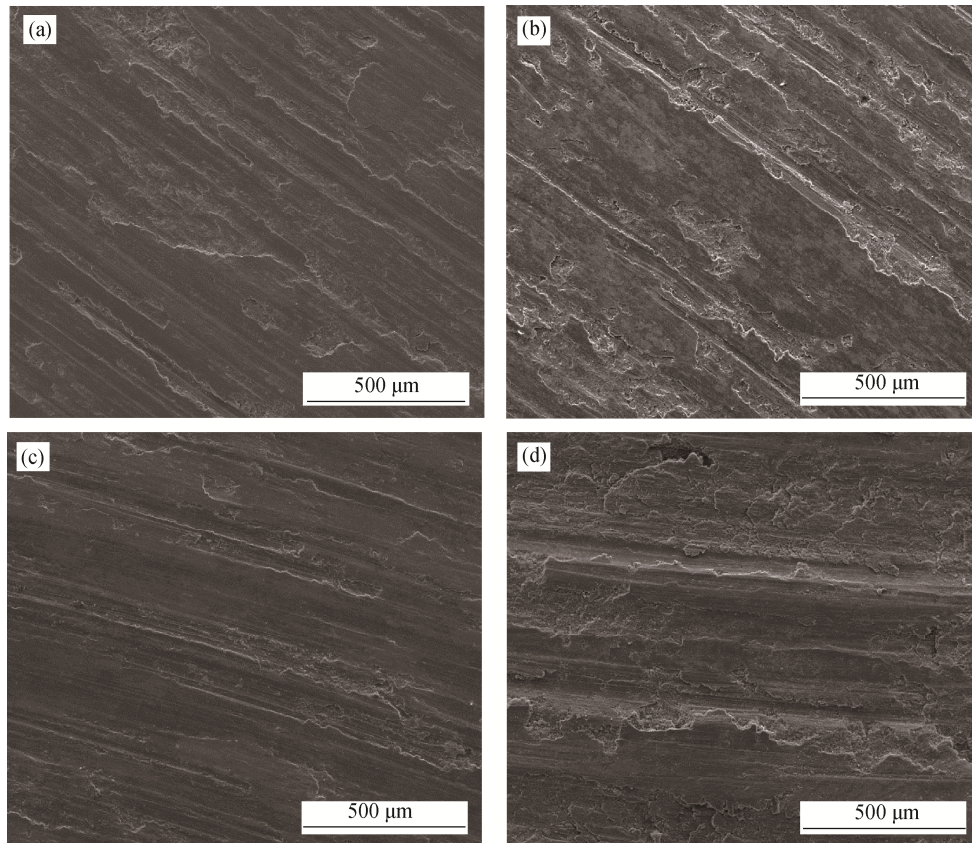


Fig. 6. Microstructures of the composite surfaces after pin-on-disc wear tests: (a) 40vol% $\text{SiC}_\text{p}/\text{Al2024}$; (b) (10vol% $\text{Al}_2\text{O}_{3\text{sf}}$ + 30vol% $\text{SiC}_\text{p})/\text{Al2024}$; (c) (20vol% $\text{Al}_2\text{O}_{3\text{sf}}$ + 20vol% $\text{SiC}_\text{p})/\text{Al2024}$; (d) (30vol% $\text{Al}_2\text{O}_{3\text{sf}}$ + 10vol% $\text{SiC}_\text{p})/\text{Al2024}$.

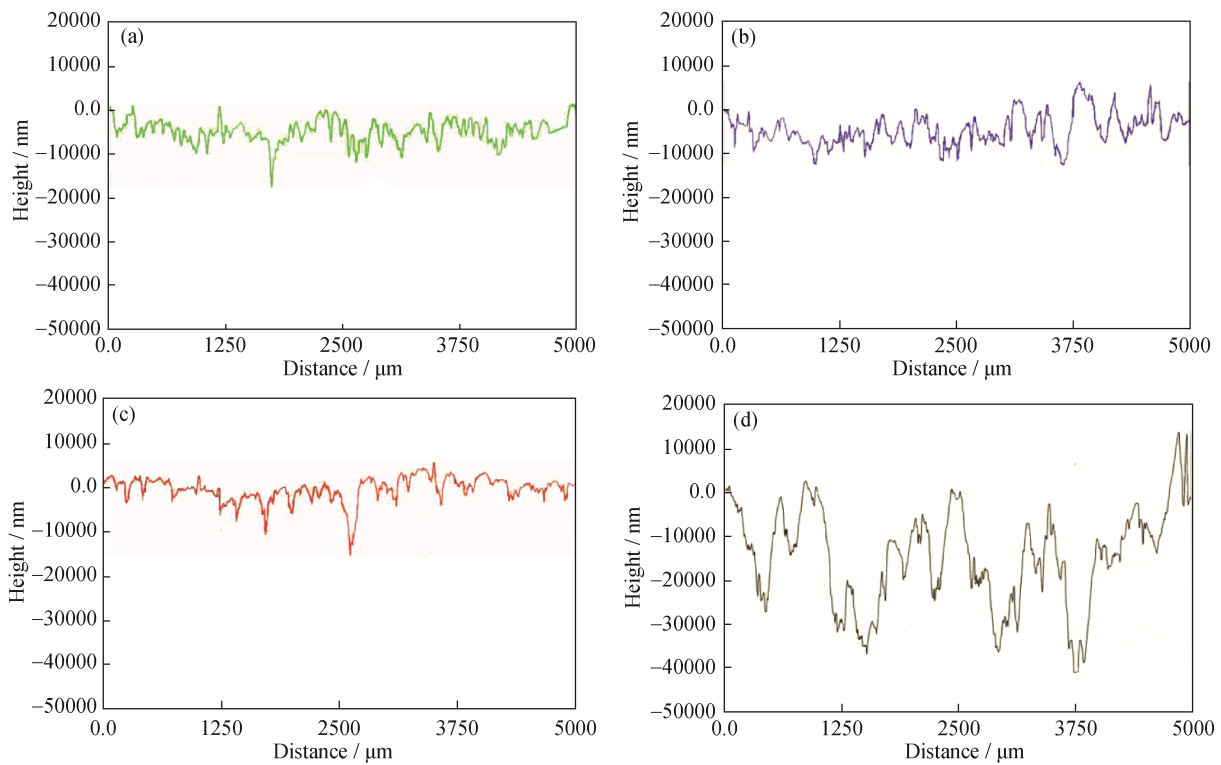


Fig. 7. Surface profiles of the samples after pin-on-disc wear tests: (a) 40vol% $\text{SiC}_\text{p}/\text{Al2024}$; (b) (10vol% $\text{Al}_2\text{O}_{3\text{sf}}$ + 30vol% $\text{SiC}_\text{p})/\text{Al2024}$; (c) (20vol% $\text{Al}_2\text{O}_{3\text{sf}}$ + 20vol% $\text{SiC}_\text{p})/\text{Al2024}$; (d) (30vol% $\text{Al}_2\text{O}_{3\text{sf}}$ + 10vol% $\text{SiC}_\text{p})/\text{Al2024}$.

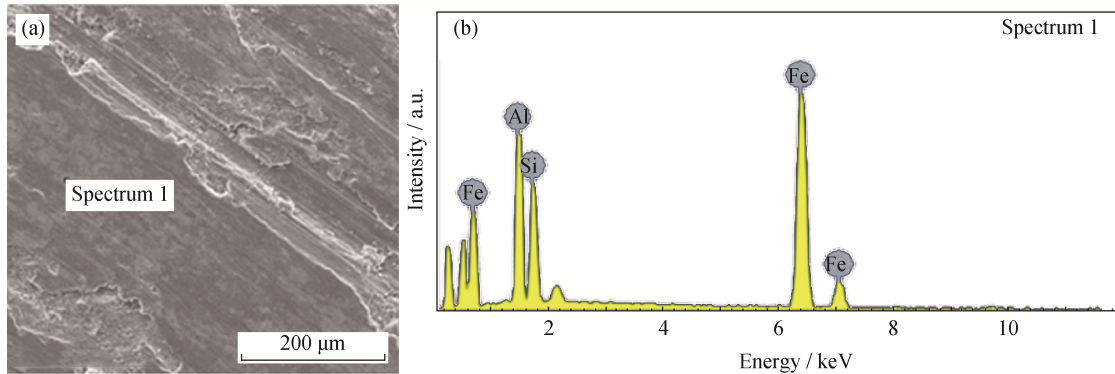


Fig. 8. Worn surface (a) and EDX spectrum (b) of the PFMMCs after pin-on-disc wear tests.

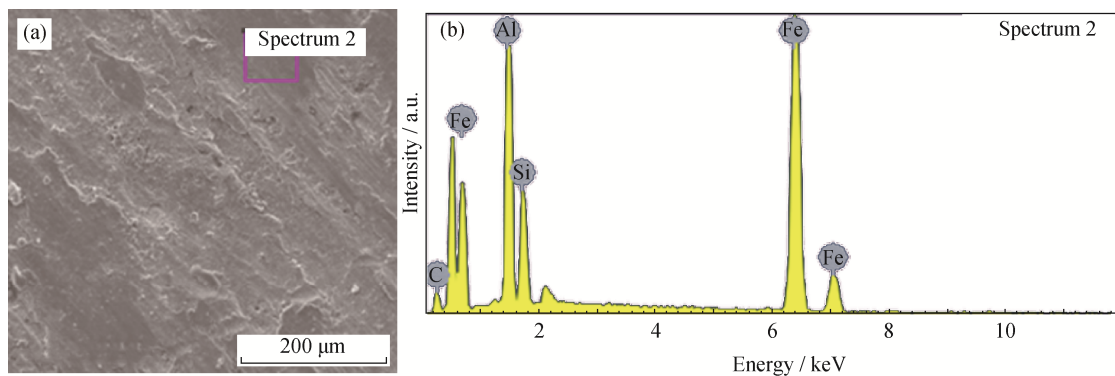


Fig. 9. Worn surface (a) and EDX spectrum (b) of HT400 after pin-on-disc wear tests.

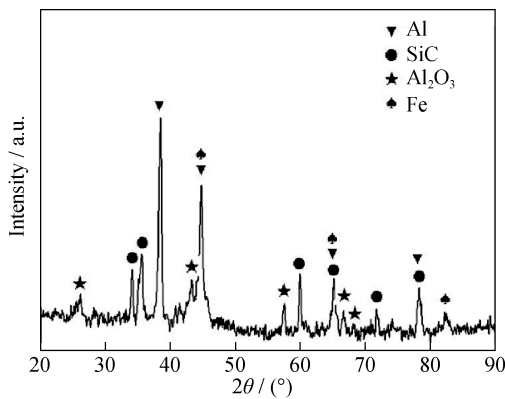


Fig. 10. XRD pattern of the PFMMCs worn surface.

3.4. Wear debris examination

Fig. 11 shows the wear debris after pin-on-disc wear tests. This wear debris mainly comes from the surface of PFMMCs and small Fe fragments from HT400. Lumpy wear debris is observed in Fig. 11(a), and its size decreases with an increase in the volume fraction of $\text{Al}_2\text{O}_{3\text{sf}}$. More and more powder-like wear debris appears, as shown in Figs. 11(b), 11(c), and 11(d). This is attributed to the fact that SiC particles drop off the matrix more easily than Al_2O_3 fibers during the process of frictional wear. Fig. 11 shows that the

shape of the desquamative SiC_p is mostly intact; however, the desquamative $\text{Al}_2\text{O}_{3\text{sf}}$ are all broken because it is more difficult to pull out than particles from the matrix. Thus, the debris decreases in size with the addition of more $\text{Al}_2\text{O}_{3\text{sf}}$. Fig. 11(d) shows that the dispersity of the debris decreases when the strengthening phase includes 30vol% $\text{Al}_2\text{O}_{3\text{sf}}$ + 10vol% SiC_p . However, the agglomeration of wear debris occurs easily during the process of adhesive wear because of higher temperatures and smaller abrasive dust particles.

4. Conclusions

As wear-resistant materials, Al2024 matrix composites reinforced with $\text{Al}_2\text{O}_{3\text{sf}}$ and SiC_p were prepared using pressure infiltration. The addition of $\text{Al}_2\text{O}_{3\text{sf}}$ could improve the compressive strength of porous preforms. The following conclusions can be drawn:

(1) When the volume ratio of $\text{Al}_2\text{O}_{3\text{sf}}$ to SiC_p was increased from 0 to 1, the K_m and COF of the composites decreased with $\text{Al}_2\text{O}_{3\text{sf}}$ addition, and the wear mechanisms were abrasive and furrow wear. When the volume ratio of $\text{Al}_2\text{O}_{3\text{sf}}$ to SiC_p increased from 1 to 3, the COF decreased continuously and the K_m increased rapidly, and the wear mechanism was adhesive wear.

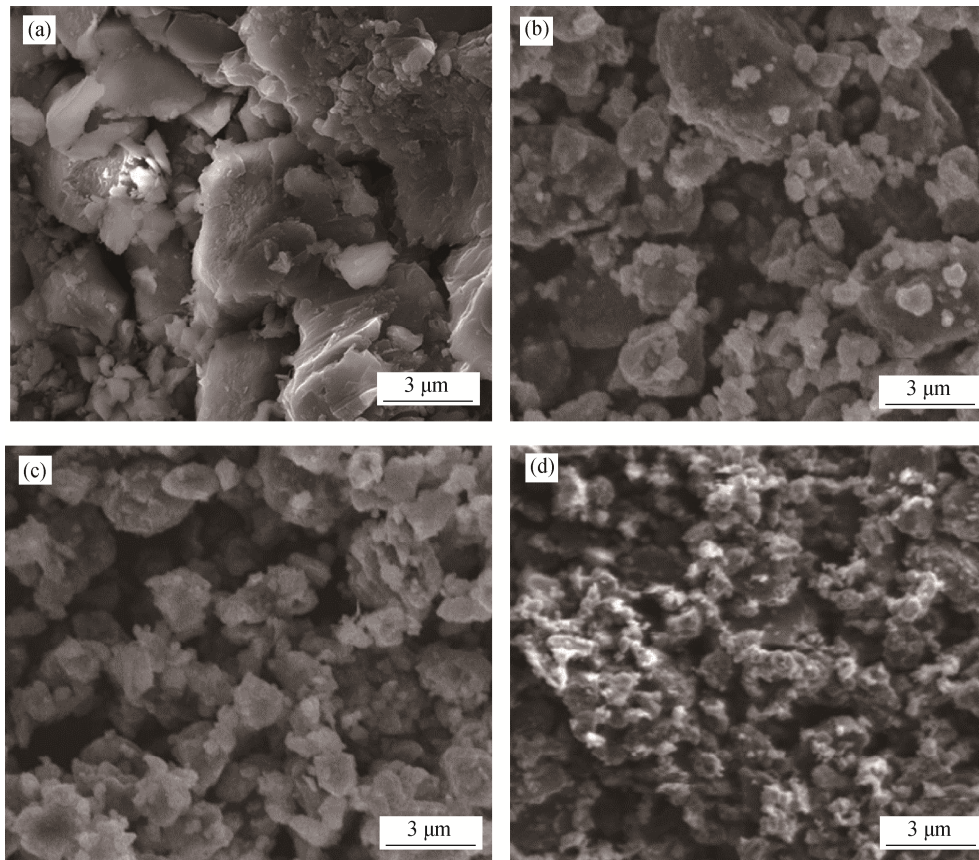


Fig. 11. SEM micrographs of wear debris after pin-on-disc wear tests: (a) 40vol% $\text{SiC}_p/\text{Al2024}$; (b) (10vol% $\text{Al}_2\text{O}_{3\text{sf}}$ + 30vol% SiC_p)/ Al2024 ; (c) (20vol% $\text{Al}_2\text{O}_{3\text{sf}}$ + 20vol% SiC_p)/ Al2024 ; (d) (30vol% $\text{Al}_2\text{O}_{3\text{sf}}$ + 10vol% SiC_p)/ Al2024 .

(2) A dense alloy layer containing Al, Fe, SiC, and Al_2O_3 was formed by mechanical alloying. The size of the wear debris decreased with an increase in the amount of $\text{Al}_2\text{O}_{3\text{sf}}$ addition.

(3) The addition of $\text{Al}_2\text{O}_{3\text{sf}}$, characterized by the ratio of $\text{Al}_2\text{O}_{3\text{sf}}$ to SiC_p , significantly affected the properties of the composites and resulted in changes in wear mechanisms. The best abrasive resistance was observed when the composition of the composite was 20vol% $\text{Al}_2\text{O}_{3\text{sf}}$ + 20vol% $\text{SiC}_p/\text{Al2024}$.

Acknowledgement

This study was financially supported by the National Natural Science Foundation of China (No. 51374028).

References

- [1] W. Cui, H. Xu, J.H. Chen, S.B. Ren, X.B. He, and X.H. Qu, Effect of graphite powder as a forming filler on the mechanical properties of SiC_p/Al composites by pressure infiltration, *Int. J. Miner. Metall. Mater.*, 23(2016), No. 5, p. 601.
- [2] G.B. Veeresh Kumar, C.S.P. Rao, and N. Selvaraj, Studies on mechanical and dry sliding wear of Al6061–SiC composites, *Composites Part B*, 43(2012), No. 3, p. 1185.
- [3] V. Kalaichelvi, D. Sivakumar, R. Karthikeyan, and K. Palanikumar, Prediction of the flow stress of 6061 Al–15% SiC–MMC composites using adaptive network based fuzzy inference system, *Mater. Des.*, 30(2009), No. 4, p. 1362.
- [4] C.G.E. Mangin, J.A. Isaacs, and J.P. Clark, MMCs for automotive engine applications, *JOM*, 48(1996), No. 2, p. 49.
- [5] J.M. Torralba, C.E. da Costa, and F. Velasco, P/M aluminum matrix composites: an overview, *J. Mater. Process. Technol.*, 133(2003), No. 1-2, p. 203.
- [6] R. Abhik, V. Umasankar, and M.A. Xavior, Evaluation of properties for Al–SiC reinforced metal matrix composite for brake pads, *Procedia Eng.*, 97(2014), p. 941.
- [7] Y.Q. Wang and J.L. Song, Dry sliding wear behavior of Al_2O_3 fiber and SiC particle reinforced aluminum based MMCs fabricated by squeeze casting method, *Trans. Non-ferrous Met. Soc. China*, 21(2011), No. 7, p. 1441.
- [8] V. Umasankar, M.A. Xavior, and S. Karthikeyan, Experimental evaluation of the influence of processing parameters on the mechanical properties of SiC particle reinforced AA6061 aluminium alloy matrix composite by powder

- processing, *J. Alloys Compd.*, 582(2014), p. 380.
- [9] L. Geng, H.W. Zhang, H.Z. Li, L.N. Guan, and L.J. Huang, Effects of Mg content on microstructure and mechanical properties of SiC_p/AlMg composites fabricated by semi-solid stirring technique, *Trans. Nonferrous Met. Soc. China*, 20(2010), No. 10, p. 1851.
- [10] R.H. Dong, W.S. Yang, Z.H. Yu, P. Wu, M. Hussain, L.T. Jiang, and G.H. Wu, Aging behavior of 6061Al matrix composite reinforced with high content SiC nanowires, *J. Alloys Compd.*, 649(2015), p. 1037.
- [11] S.W. Lai and D.D.L. Chung, Fabrication of particulate aluminum-matrix composites by liquid-metal infiltration, *J. Mater. Sci.*, 29(1994), No. 12, p. 3128.
- [12] N.P. Cheng, S.M. Zeng, and Z.Y. Liu, Preparation, microstructures and deformation behavior of SiC_p/6066Al composites produced by PM route, *J. Mater. Process. Technol.*, 202(2008), No.1-3, p. 27.
- [13] S. Black, Metal-matrix composites used to lighten military brake drums, *High Perform. Compos.*, 18(2010), No. 3, p. 101.
- [14] J.L. Young Jr., D. Kuhlmann-Wilsdorf, and R. Hull, The generation of mechanically mixed layers (MMLs) during sliding contact and the effects of lubricant thereon, *Wear*, 246(2000), No. 1-2, p. 74.
- [15] B.N. Pramila Bai and S.K. Biswas, Effect of magnesium addition and heat treatment on mild wear of hypoeutectic aluminium-silicon alloys, *Acta Metall. Mater.*, 39(1991), No. 5, p. 833.
- [16] B. Venkataraman and G. Sundararajan, Correlation between the characteristics of the mechanically mixed layer and wear behaviour of aluminum, Al-7075 alloy and Al-MMCs, *Wear*, 245(2000), No. 1-2, p. 22.